Proceedings of the 21st ICSMGE, Vienna, Austria, 14 – 19 June 2026. Pistrol, Adam & Schweiger (eds.)
Published by: ÖGG, Austrian Society for Geomechanics, Salzburg, Austria, ISBN 978-3-9503898-4-5
https://doi.org/10.53243/ICSMGE2026-1746

Numerical Investigation on Dynamic Response of Disconnected Piled Raft Foundation in Liquefiable Soil

Ankit Kumar Suman, Rajeswari J.S.
Department of Civil Engineering, School of Infrastructure, Indian Institute of Technology Bhubaneswar, Khordha, Odisha, India, a23ce09008@iitbbs.ac.in

ABSTRACT: In earthquake-prone regions, liquefaction-induced ground deformation poses a critical challenge to foundation design. Disconnected piled raft (DPR) foundations offer a promising solution by mitigating settlements while significantly reducing bending moments and shear forces at the pile head compared to conventional piled raft systems. This innovative approach, which primarily utilizes piles as settlement reducers, enhances seismic performance and ensures structural safety under dynamic loading. This study investigates the behaviour of DPR foundations in liquefiable soils through three-dimensional numerical modelling in a finite difference-based computer program, *FLAC 3D*. The soil profile contains a partially liquefiable sand layer confined between dense non-liquefiable layers, representing a common field condition where deep foundations are used to bypass weak strata. A built-in Finn constitutive model, incorporating the Martin and Byrne relationships into the Mohr-Coulomb framework, is employed to accurately simulate the cyclic response of sand. The numerical model is validated against shake table test data to ensure reliability. The model is then subjected to earthquake base excitation to evaluate the performance of DPR against seismic loading. Results reveal that DPR foundations effectively reduce bending moments and axial forces at the pile head. The inclusion of a cushion layer can further enhance the system's ability to distribute loads and dissipate seismic energy, underscoring its efficiency as an earthquake-resistant foundation design. These findings highlight the potential of DPR foundations as a sustainable and efficient solution for mitigating the adverse effects of soil liquefaction in seismic regions.

KEYWORDS: Disconnected piled raft foundation, Liquefaction, Numerical modelling.

1 INTRODUCTION

A loose to medium-saturated sand is prone to liquefaction under seismic loading, where a temporary loss of effective stresses and a sharp drop in soil stiffness and shear strength are observed due to the build-up of excess pore water pressure. This is a common phenomenon that has been responsible for significant foundation failures, particularly in coastal and alluvial regions. Over the past few decades, extensive research has been conducted on the seismic behavior of pile groups and pile foundations in liquefiable soils. Knappett and Madabhushi (2008) reported that pile groups in liquefiable and laterally spreading soils are subjected to large settlements and differential settlements. This is due to loss of soil stiffness and kinematic loading. Hussein and El Naggar (2021) further found that the axial load-transfer mechanism of the pile groups changes drastically in liquefiable deposits with sufficient reduction in the shaft resistance and load distribution along the pile length. Xu et al. (2020) conducted a large-scale shake table test and provided direct experimental evidence that there are different behaviors in pile group structures when they are in liquefiable versus non-liquefiable soil layers. This emphasizes the importance of accounting for soil layering, degree of liquefaction, and dynamic soil-structure interaction in the study.

For structures that are heavy and sensitive to excessive settlements, traditional pile foundations have been adopted in the liquefiable zones. However, in recent decades, piled raft foundations have gained attention for their potential to optimise material usage while improving load-sharing behaviour between the piles and the raft. Historic earthquakes such as the 1964 Niigata, 1989 Loma Prieta, and 1995 Kobe events have shown multiple cases where the foundations are severely distressed due to liquefaction. For structures in such soils, deep foundations such as piled rafts are often used to bypass the weak strata. Two distinct piled raft configurations have been recognized. In the connected piled raft foundations (CPRFs), piles are rigidly connected to the raft, ensuring simultaneous load transfer. However, due to the rigid connection between the piles and the raft, high bending moments and shear forces are observed in the piles. This led to the introduction of disconnected piled raft foundations (DPRFs), where the piles are detached from the raft, and a granular cushion layer is introduced between the piles and the raft, allowing the raft-soil system to mobilize first, thereby delaying the pile engagement. This also reduces the pile forces under static and dynamic loading (Azizkandi et al. 2020). In the early days, research on piled raft foundations was mainly focused on static conditions. Poulos (2001) and Reul and Randolf (2004) explored the geotechnical and economic benefits of the CPRFs for high-rise buildings, while Horikoshi et al. (2023) studied the dynamic response of piled raft foundations in non-liquefiable soil using centrifuge and shake table tests. Chatterjee et al. (2019) conducted a numerical study on the behavior of piles in liquefiable soil, focusing on the effects of pile spacing, length, and stiffness. Bhadury et al. (2020) conducted a numerical study using *FLAC 3D*, in which connected piled raft foundations and conventional pile groups were modeled in a three-layered soil profile with a liquefiable Nevada sand layer, and their performances were compared. The result highlighted that CPRFs developed 35-70% higher pile resistance, and reduced excess pore water pressure (EPWP) ratios were observed. Maheshwari and Firoz (2024) emphasized the importance of realistically simulating pore pressure generation and dissipation when modeling CPRFs in liquefiable soils. They also studied the settlement response of CPRF for NPP structures in both liquefiable and non-liquefiable soils (Maheshwari and Firoz, 2023). Similarly, Rajeswari and Sarkar (2021) conducted a dynamic study of batter piles in liquefiable soil, incorporating the effect of variable permeability during liquefaction. The newly published IS 19117:2025 (Design and Construction of Combined Piled-Raft Foundations) discusses the use of the piled-raft system and acknowledges its suitability for medium- to heavy-load structures. The code suggests using CPRF as a foundation in a seismic area, provided that there are no weak or liquefiable layers immediately below the raft, and the piles are capable of transferring the loads safely to the competent strata.

In the present study, the soil profile does not represent a fully liquefiable deposit. Instead, the liquefiable stratum consists of a loose sand layer that is sandwiched between dense, non-liquefiable sands at the top and bottom. Such layered configurations are common in natural alluvial deposits and

reclaimed coastal fills, where liquefaction occurs only within intermediate pockets of loose sand while the surrounding dense layers provide confinement. In practice, deep foundations are routinely adopted in these conditions to bypass the liquefiable layer and transfer loads to the competent dense stratum below. Although few studies exist in which the performance of CPRFs in liquefiable soil has been studied under dynamic loading, similar studies have not yet been found for disconnected piled raft foundations, and it remains unexplored. This study explores the performance of a disconnected piled raft foundation in liquefiable soil under earthquake loading, and the results are compared with those of a connected piled raft foundation under similar conditions.

2 NUMERICAL MODELLING

2.1 *Modelling of Foundation System*

The numerical model was created in *FLAC 3D*, where the soil, cushion layer, and raft were modelled using 8-noded hexahedral grid elements, and the piles were modelled using 2-noded pile structural elements with 6 degrees of freedom per node, capturing bending, shear, and axial response for accurate displacement and stress distribution under loading. The meshing was optimised to balance the accuracy and the computational efficiency, and the size of the element was less than one-tenth of the wavelength associated with the predominant period of the input motion. The soil domain was modelled with dimensions 49m x 35m x 30m, ensuring the boundary effects were minimised. The soil layer consists of a cushion layer (1m) at the top, followed by a dense Nevada sand layer of 3m thickness with 80% relative density.

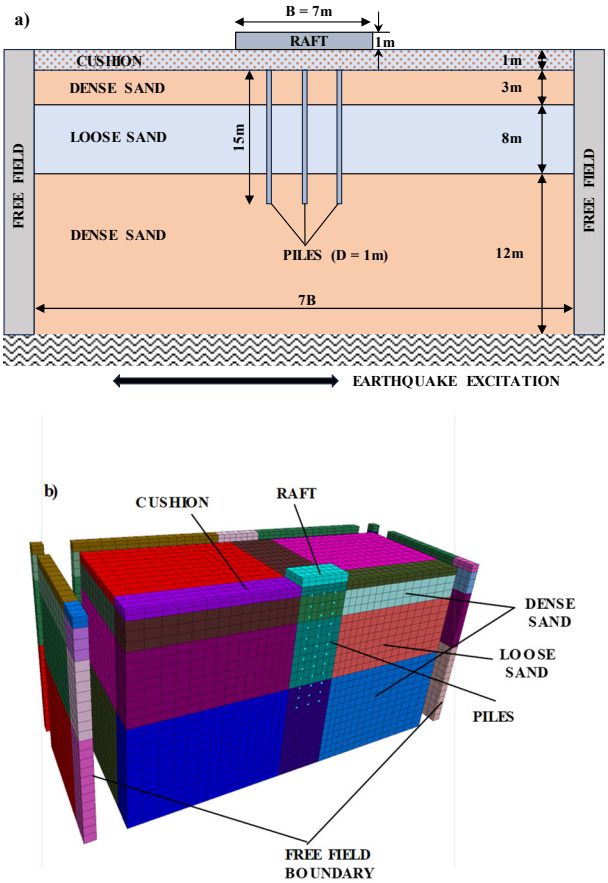

Figure 1. (a) Schematic diagram (b) Finite difference meshing of the DPR model used in the study.

Then there is a loose Nevada sand layer (40% relative density) spanning up to 8m thickness, and the bottom layer is again a dense Nevada sand layer with 80% relative density. The cushion layer is also the same dense Nevada sand layer, but then the stiffness of the cushion layer is further varied to see its effect on the peak acceleration at the raft top. The schematic diagram of the system and the numerical finite difference meshing of the model are shown in Figure 1. The inelastic behaviour of the non-liquefiable soils was modelled using the Mohr-Coulomb model, which assumes an elastic-perfectly plastic behaviour of the soil, and the liquefiable soil was modelled by using the Finn model, as implemented in the *FLAC 3D* constitutive library. This model is useful in simulating the pore water pressure generation during the cyclic loading. This model is built upon the Mohr-Coulomb framework, which incorporates the pore pressure generation formulation proposed by Byrne (1991). In this study, a square raft of size 7 meters and thickness of 1 meter was used, and the piles had a length of 15 m and a diameter of 0.6 m. Both the raft and piles were simulated using a linear-elastic constitutive model. All the material properties used in the analysis are summarised in Tables 1 and 2.

Table 1. Material properties of soil and cushion layer (Rahmani and Pak 2012).

Parameter	Unit	Loose sand	Dense sand
RD	%	40	80
Density	kg/m^3	1957	2052
Shear modulus (G)	MPa	27.1	41.9
Bulk modulus (K)	MPa	70.4	109.26
$(N_1)_{60}$	--	7	28
Porosity	--	0.424	0.373

Interfaces were defined between the raft and the cushion layer and the pile and soil to simulate the realistic load transfer and interaction effects. These interfaces were assigned normal and shear stiffness values to replicate the frictional behavior at each contact. The interaction properties of the pile elements were available in the program as normal and shear coupling stiffness (k_n and k_s respectively), which were adopted based on the guidelines provided by Timoshenko and Goodier and were helpful in predicting the pile element's sliding and separation (Chatterjee et al. 2019).

$$k_s = \frac{32 + (1-\mu) \times G_s \times r}{7 + 8 \times \mu} \quad (1)$$

$$k_n = \frac{4 \times G_s \times r}{1 - \mu} \quad (2)$$

Where, k_s = shear coupling stiffness of the soil-pile interface, k_n = normal coupling stiffness of the soil-pile interface, G_s = shear modulus of the soil, and r = radius of the pile.

Table 2. Material and geometrical properties of the raft and piles.

Parameter	Unit	Raft	Pile
Size	m	7 x 7 x 1	0.6(D) x 15(L)
Density	kg/m^3	2500	2500
Young's modulus (E)	GPa	25	25
Poisson's ratio (v)	--	0.2	0.2

2.2 *Validation*

For the validation of the model developed and the procedure followed, two different sets of shake table test data were taken, which were conducted by Horikoshi et al. (2003) and Taboada and Dobry (1993). In case 1, a sinusoidal excitation was at the base of the model, which consisted of a piled raft system with a raft (4 m x 4 m x 3 m) and piles (diameter = 0.5 m and length = 9 m) in a 3 x 3 configuration. The superstructure was also modelled as a volume element to replicate the loading of a realistic structure as described in the work. The input motion consisted of a sinusoidal wave with an amplitude of 1 m/s^2 and a frequency of 1 Hz, which replicated the experimental test parameters. The output acceleration at the raft top was compared with that obtained from the experiment. It can be seen from Figure 2 that the comparison revealed a strong agreement between the simulated and observed responses, which indicated that the numerical model can replicate the seismic behaviour of the piled raft foundation under dynamic loading.

The second case represents a shake table test conducted by Taboada and Dobry (1993), which consisted of saturated Neveda sand of 40% relative density, and it was subjected to a centrifuge acceleration of 50 g. The 10 m-high uniform sand deposit (prototype scale) was subjected to base shaking using

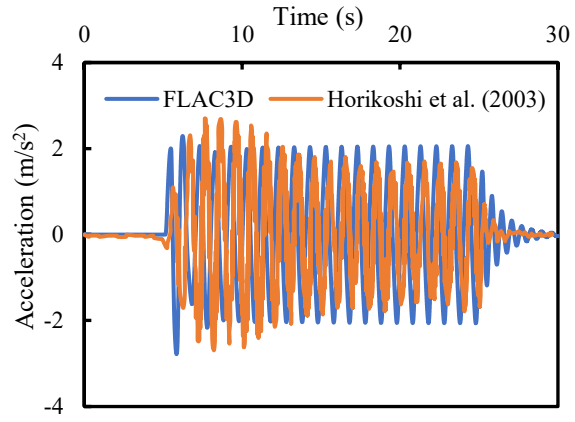

Figure 2. Comparison of output acceleration at the raft top.

an input accelerogram with a peak ground acceleration (PGA) of 0.23 g. The variation of excess pore water pressure at 1.45 m below the top surface obtained from the software and the experiment is compared in Figure 3. As can be seen from the figure, the results match reasonably well, indicating the capability of the model to reliably replicate the excess pore water pressure developed within the model.

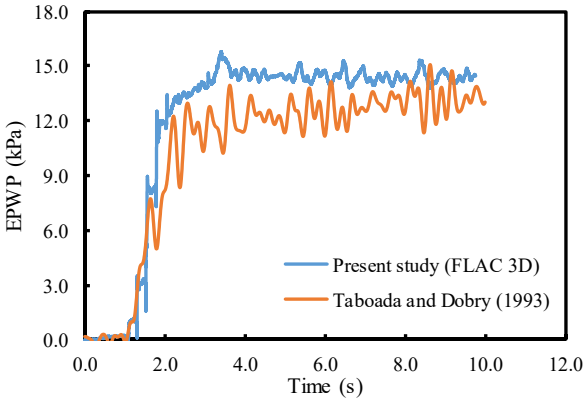

Figure 3. Comparison of excess pore water pressure developed in the liquefiable sand.

3 GROUND MOTION

The seismic loading applied in this study is based on a recorded acceleration time history from the 1994 Northridge earthquake, which had a moment magnitude of 6.69. The selected ground motion was recorded at the Castaic-Old Ridge Route station, located approximately 20.72 km from the earthquake's epicenter. This ground motion was chosen due to its high intensity and well-documented characteristics, making it suitable for evaluating the seismic response of soil–foundation–structure systems. The input motion has a peak ground acceleration (PGA) of 0.568g and a predominant period of 0.26 seconds.

4 RESULTS AND DISCUSSIONS

In this study, an attempt has been made to compare the forces generated in the pile for connected and disconnected piled raft foundations in liquefiable soil. For this, the numerical model is prepared and is validated with the already published results. Then the model is subjected to vertical loading, which is equal to 50% of the ultimate vertical capacity of the DPRF, and the model is brought to equilibrium. Further, the earthquake time history, as mentioned in section 3, was applied at the base.

4.1 *Acceleration response at the raft top*

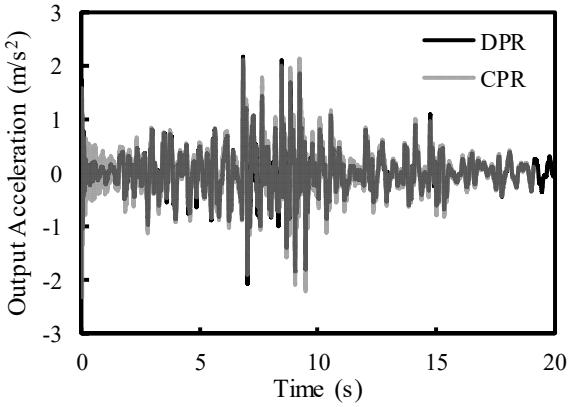

Figure 4. Output acceleration time history for CPR and DPR at the raft top.

Figure 4 presents the acceleration time histories recorded at the raft top for both disconnected piled raft and connected piled raft systems. The thickness of the cushion layer for this study is 1m, and the properties are the same as those of dense Nevada sand. It can be noted from the figure that the output acceleration is slightly lower in the case of a disconnected piled raft, particularly between 6 s and 12 s, whereas CPR exhibits slightly higher peak acceleration. This may be due to the absence of the rigid pile-raft connectivity, which allows for the partial isolation of the raft from the pile-induced vibrations. Consequently, the DPR exhibits a slightly improved ability to dissipate seismic energy at the raft location, thereby reducing the intensity of the acceleration transmitted to the superstructure.

4.2 *Excess pore water pressure ratio*

Figure 5 represents the excess pore water pressure ratio (r_u) at three depths within the liquefiable soil layer (z = -5, -8, and -11 m) at the free field location. At all depths, r_u rises sharply, which indicates that there is a rapid rise in the pore water pressure generation under cyclic loading. In the liquefiable layer, r_u reaches close to 1, and then it stabilizes with little fluctuations. It suggests that there is sustained liquefaction occurring in this layer, and since there is slightly higher confinement as the

location is deeper, this limits the pore water pressure dissipation. Overall, the highest dissipation is seen in the upper region, as there might be drainage proximity, while the deeper layer retains the elevated r_u for longer durations.

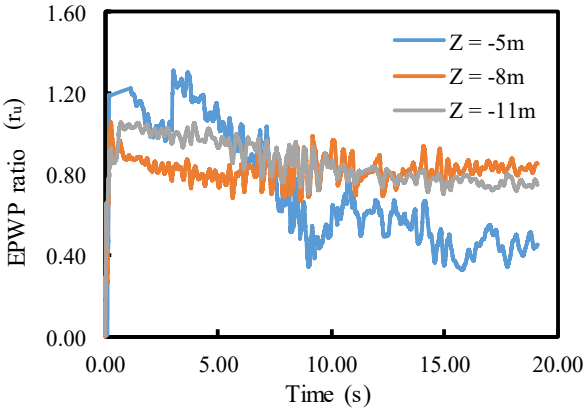

Figure 5. Excess pore water pressure ratio within the liquefiable sand layer.

4.3 *Axial forces in piles*

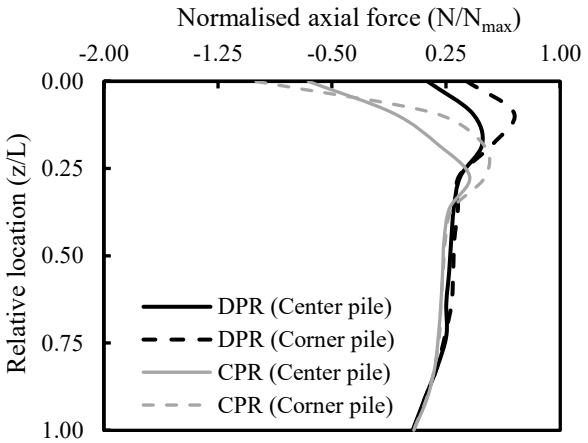

Figure 6. Comparison of axial forces in the piles in CPR and DPR.

Axial forces in the piles are one of the most important aspects to compare when analyzing a disconnected piled raft. Figure 6 compares the normalized axial force profiles along the center and corner piles for both the DPR and CPR systems. It can be clearly seen from the figure that the piles carry higher axial loads in the case of CPR compared to DPR, indicating more direct load transfer through the rigid connectivity between the raft and the piles. Additionally, the corner piles exhibit slightly higher axial forces at the top compared to the center pile in both cases. However, a relatively uniform load distribution is observed in the DPR case between the center and corner piles, with lower peak forces near the head and a smoother reduction with depth. This behaviour in the DPR is due to the absence of a rigid connection between the raft and piles, which allows part of the raft load to be redistributed to the surrounding soil before engaging the piles, thereby reducing the immediate axial demands on the individual piles.

4.4 *Shear forces in piles*

As expected, the maximum shear forces occur near the pile head, which gradually reduce with depth and approach zero at the pile toe. As shown in Figure 7, higher shear forces are experienced near the pile head, with a noticeable peak within the top quarter of the pile length in the case of CPR. This indicated that there is a greater transfer of the lateral loads in the piles due to the rigid connection. In contrast, the DPR experiences relatively lower peak shear forces in the piles because there is an absence of a direct pile-raft connection, which allows part of the seismic-induced lateral demands to be redistributed to the surrounding soil, thereby limiting the abrupt shear peak in the piles. Also, it can be observed that the corner piles experience a greater shear force than the center piles, which is likely due to the edge effect.

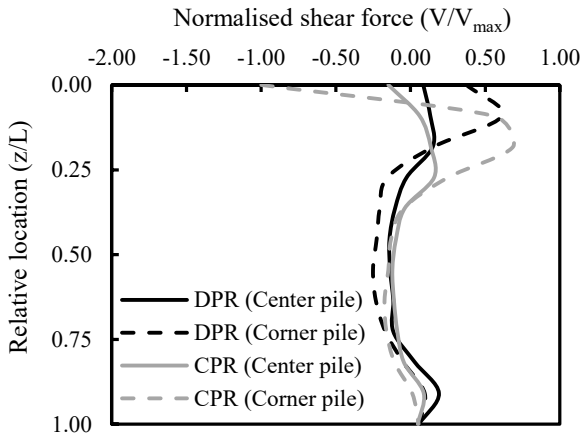

Figure 7. Comparison of shear forces in the piles in CPR and DPR.

4.5 *Bending Moments in Piles*

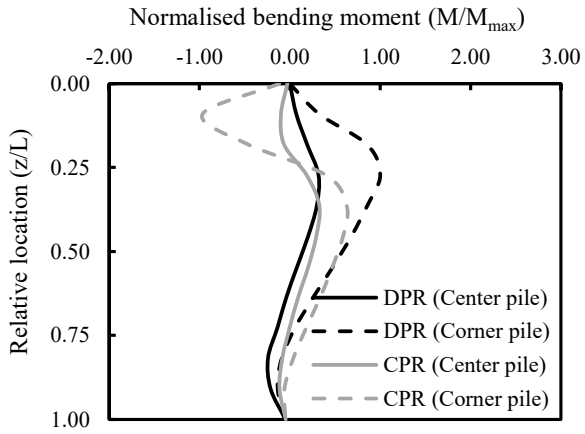

Figure 8. Bending moment profile in the piles in CPR and DPR.

Figure 8 represents the bending moment profiles for the center and corner piles in both the disconnected piled raft and connected piled raft systems. It can be noted that the bending moments are more concentrated in the upper portion of the piles, with the peak value being experienced within the top third of the pile length. The bending moment experienced by the piles in CPR is higher compared to that of DPR, and the peak value occurs at approximately 20-30% of the pile length from the head. This behaviour is consistent with the fact that there is a more rigid transfer of the lateral and rotational load from the raft into the piles, which amplifies the bending demands near the pile head. The center piles also experience the same behaviour, but it is slightly lower than that of the corner piles. On the contrary, bending moments are generally lower across the pile length in the case of DPR, where the absence of a direct raft-pile connection reduces the transfer of abrupt rotational and lateral loads into the pile head, suggesting that the DPR configuration offers improved resistance against overstressing in the piles under seismic excitation.

4.6 *Effect of cushion thickness*

Figure 9 represents the variation in maximum acceleration at the raft top when the thickness of the cushion layer is varied in the disconnected piled raft configuration. Here, the properties of the cushion layer are the same as in section 4.1. The thickness of the cushion layer is represented by the cushion-to-raft thickness ratio (t_c/t_r). From the figure, a clear decreasing trend is observed as the thickness of the cushion layer is increased. When t_c/t_r =1.0, the maximum acceleration transmitted to the raft is approximately 2.2 m/s². However, when t_c/t_r is increased to 2, a reduction in the maximum acceleration to around 1.4 m/s² (36% reduction) was observed at the raft top. This progressive reduction demonstrates the effectiveness of the cushion layer in filtering high-frequency seismic energy and reducing the stiffness of the raft-pile connection. A thicker cushion layer introduces additional compliance at the raft–soil interface, allowing greater relative movement between the raft and the pile heads and thereby minimizing the direct transmission of inertial forces.

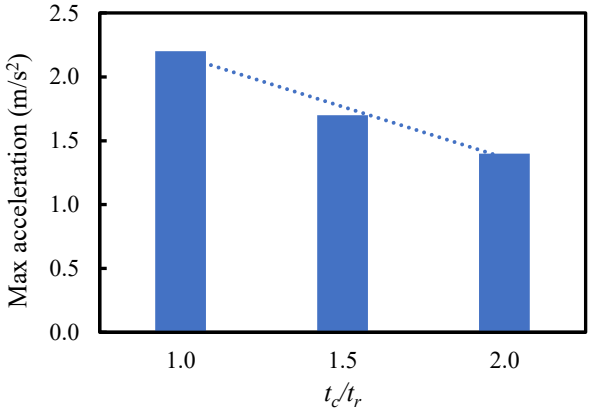

Figure 9. Effect of cushion thickness on the peak acceleration at the raft top.

Variation in the cushion thickness also affects the lateral displacement of the raft. Figure 10 shows the variation of maximum lateral displacement measured at the raft top during the shaking period for different cushion thicknesses. A consistent decrease in lateral displacement was noted as the cushion thickness increased. When the cushion thickness ratio (t) = 1.0, the raft was subjected to a maximum lateral displacement of around 80mm. Increasing the thickness ratio to t = 2 lowers the peak displacement to about 65 mm.

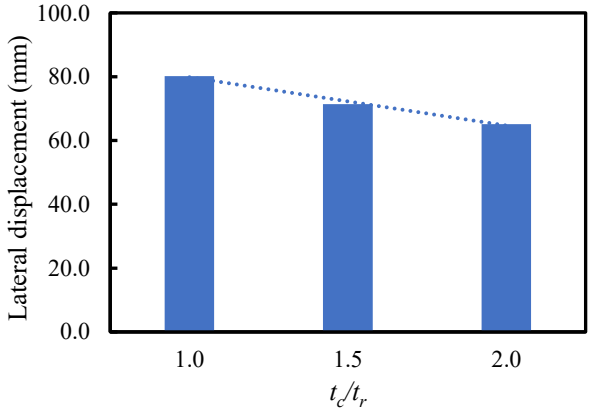

Figure 10. Effect of cushion thickness on the maximum lateral displacement measured at the raft top.

This behaviour arises from the improved seismic isolation afforded by a thicker cushion. In the disconnected piled raft configuration, the cushion plays a crucial role, governing the transfer of horizontal inertial forces from the soil below to the raft. A thicker cushion allows for greater deformability and attenuates the high-frequency components of the ground motion, thereby reducing the kinematic forces transmitted to the raft. A thicker cushion also delays the mobilisation of the pile resistance, which prevents the axial forces at the pile-head and decreases the overall lateral drift.

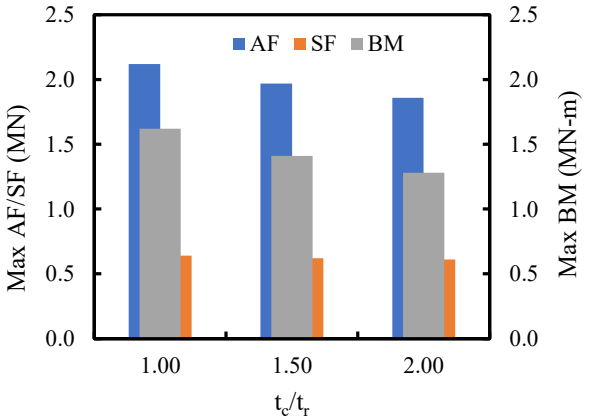

Figure 11. Effect of cushion thickness on the pile forces and bending moment.

Figure 11 illustrates the variation of maximum axial force (AF), shear force (SF), and bending moment (BM) in the piles as the thickness of the cushion layer is varied. A consistent decrease in all three force components was noted as the cushion thickness was increased. At t = 1, the highest demands were experienced by the piles, and increasing the thickness to t = 2 resulted in a noticeable reduction in the AF and BM values among the three cases; however, there was only a slight reduction in the shear forces in the piles. This reflects the beneficial effect of the increased separation between the raft and the pile heads. The observed trends demonstrate the crucial role of the cushion layer in regulating the degree of raft-pile interaction under dynamic loading. When there is a thicker cushion, it introduces additional compliance, which delays the direct mobilization of the pile resistance and hence reduces the kinematic and inertial load transfer to the piles during shaking. The decrease in the values is particularly significant for axial forces and bending moments, which are highly sensitive to the raft and soil movements under seismic excitation. The decrease in bending moment with increasing cushion thickness suggests that the cushion effectively mitigates rotational demand and reduces the stiffness contrast at the pile head, thereby lowering the curvature-induced stresses.

5 CONCLUSIONS

In this study, the seismic performance of disconnected piled raft (DPR) and connected piled raft (CPR) foundations in liquefiable soil is compared using three-dimensional numerical analysis in *FLAC 3D*. Both systems exhibited a rapid buildup of excess pore water pressure where r_u approached unity early in the shaking. An increase in the thickness of the cushion layer helped reduce the transmission of high-frequency components of the input motion, resulting in a consistent decrease in both the maximum acceleration at the raft top and the lateral displacement of the raft. Increasing the cushion thickness consistently reduced the maximum axial force, shear force, and bending moment in the piles by moderating raft-pile interaction and filtering seismic energy. Hence, cushion characteristics strongly influence the dynamic soil-structure interaction in the disconnected piled raft foundations and their careful selection

can significantly enhance the seismic performance, The axial load, shear forces, and bending moment profiles showed that the DPR can effectively reduce the pile structural demands under the seismic loading in liquefiable soil as compared to CPR, making them a promising alternative to the conventional CPR system, although the potential implications for long-term settlement require further study.

6 REFERENCES

Azizkandi, A.S., Aghamolaei, M. and Hasanaklou, S.H., 2020. Evaluation of dynamic response of connected and non-connected piled raft systems using shaking table tests. *Soil Dynamics and Earthquake Engineering*, *139*, p.106366.

Bhaduri, A., Rao, V.D. and Choudhury, D., 2020. The behaviour of pile group and combined piled-raft foundation in liquefiable soil under seismic conditions. *Geotechnical Engineering Journal of the SEAGS & AGSSEA*, *51*(2), pp.130-138.

Chatterjee, K., Choudhury, D., Rao, V.D. and Poulos, H.G., 2019. Seismic response of single piles in liquefiable soil considering P-delta effect. *Bulletin of Earthquake Engineering*, *17*(6), pp.2935.

Hussein, A.F. and El Naggar, M.H., 2021. Seismic axial behaviour of pile groups in non-liquefiable and liquefiable soils. *Soil Dynamics and Earthquake Engineering*, *149*, p.106853.

Horikoshi, K., Matsumoto, T., Hashizume, Y. and Watanabe, T., 2003. Performance of piled raft foundations subjected to dynamic loading. *International Journal of Physical Modelling in Geotechnics*, *3*(2), pp.51-62.

Indian Standard: 19117: 2025 Design and construction of combined piled-raft foundations-code of practice. *Bureau of Indian Standards, New Delhi*.

Knappett, J.A. and Madabhushi, S.P., 2008. Liquefaction-induced settlement of pile groups in liquefiable and laterally spreading soils. *Journal of geotechnical and geoenvironmental engineering*, *134*(11), pp.1609-1618.

Maheshwari, B.K. and Firoj, M., 2023. Settlement of combined piled raft foundation of a nuclear power plant in non-liquefiable and liquefiable soils. *Nuclear Engineering and Design*, *413*, p.112518.

Maheshwari, B.K. and Firoj, M., 2024. Seismic response of combined piled raft foundation using advanced liquefaction model. *Soil Dynamics and Earthquake Engineering*, *181*, p.108694.

Poulos, H.G., 2001. Piled raft foundations: design and applications. *Geotechnique*, *51*(2), pp.95-113.

Rahmani, A. and Pak, A., 2012. Dynamic behavior of pile foundations under cyclic loading in liquefiable soils. *Computers and Geotechnics*, *40*, pp.114-126.

Rajeswari, J.S. and Sarkar, R., 2021. Seismic behavior of batter pile groups embedded in liquefiable soil. *Earthquake Engineering and Engineering Vibration*, *20*(3), pp.583-604.

Reul, O. and Randolph, M.F., 2004. Design strategies for piled rafts subjected to nonuniform vertical loading. *Journal of Geotechnical and Geoenvironmental Engineering*, *130*(1), pp.1-13.

Xu, C., Dou, P., Du, X., El Naggar, M.H., Miyajima, M. and Chen, S., 2020. Seismic performance of pile group-structure system in liquefiable and non-liquefiable soil from large-scale shake table tests. *Soil Dynamics and Earthquake Engineering*, *138*, p.106299.